Open Ceramics 13 (2023) 100319

Contents lists available at ScienceDirect

Open Ceramics

journal homepage: www.sciencedirect.com/journal/open-ceramics

Field assisted sintering of Ta–Al_2O_3 composite materials and investigation of electrical conductivity

Bastian Kraft *, Susanne Wagner, Karl G. Schell, Michael J. Hoffmann

Karlsruhe Institute of Technology, Haid-und-Neu-Str. 7, 76131, Karlsruhe, Germany

ARTICLE INFO

Keywords:
Field assisted sintering
Refractory composite
Electrical conductivity
Microstructure
Alumina
Tantalum

ABSTRACT

Ta–Al_2O_3 composite samples with different compositions are prepared using Field Assisted Sintering Technique (FAST). Two different alumina powders are used to investigate the influence of the starting powders particle size on the microstructural features and the resulting electrical conductivity of the prepared composite materials. Percolation threshold of the two material systems is influenced by the metal fraction, as well as the alumina particle size of the starting powder. The percolation threshold for the fine- and the coarse-grained alumina is found to be at 15 vol.-% Ta and 7.5 vol.-% Ta, respectively. Microstructural investigations show significant differences in terms of particle shape of both, Ta and Al_2O_3 after sintering, most likely being the reason for the different percolation thresholds of the investigated materials. Anisotropy effects resulting from the processing using FAST and the influence on electrical properties are also shown.

1. Introduction

This work is part of an interdisciplinary research group with the main objective to develop coarse-grained refractory ceramic-metal composites and to analyze the corresponding material properties. To achieve this goal a two-step process is being proposed: In the first step fine-grained powder mixtures are processed to prepare dense and porous samples for crushing. The resulting coarse-grained "particles", which already consist of a ceramic-metal composite, are then again processed and densified using different pressure-assisted and pressureless sintering techniques. The new class of materials is considered to be used as refractories in the foundry technology. Therefore, coarse microstructures are of interest due to their creep resistance, their good thermal shock resistance due to porosity and the low shrinkage during the final sintering step [1–4]. The improved thermal shock resistance of coarse microstructures is a result of a microcrack network. The porosity prevents crack propagation and reduces the Young's modulus, which is also favorable in terms of thermal shock resistance [5,6]. A lot of research is done on processing of fine-grained composites, whereas the coarse-grained attempt with pre-synthesized particles followed here is new in the field of refractories. In this study we analyze the influence of particle size of both, the alumina raw powder and different Ta–Al_2O_3 material compositions after the first densification step using Field Assisted Sintering Technique (FAST) to achieve a basic understanding of the microstructure-property relationship with special emphasis on the electrical conductivity with respect to the development of direct heatable components. Such components are for example considered as pre-heatable heatshields in gas turbines, to reduce thermal stresses during startup and to increase their durability. State of the art for such components like heatshields is mullite containing Al_2O_3, where the decomposition of mullite under reducing atmosphere at 1300 °C limits the application temperature. The findings of this research are the first investigations of processing Ta–Al_2O_3 using FAST and will be used to identify most suitable material systems and compositions for optimization of material costs, favorable material density and electrical conductivity, depending on the applicational interests.

The findings presented in this study are complementary to the findings in Ref. [7] and show the effects of replacing refractory metal Nb by Ta. Due to its higher melting point, tantalum is considered to be suitable for applications with higher thermal stresses compared to niobium and therefore allows higher application temperatures of the composites. The investigations here show the first approach of field assisted sintering of Ta–Al_2O_3 composites and the investigations of electrical conductivity depending on the material composition.

* Corresponding author.
E-mail addresses: Bastian.Kraft@kit.edu (B. Kraft), Susanne.Wagner@kit.edu (S. Wagner), Guenter.Schell@kit.edu (K.G. Schell), Michael.Hoffmann@kit.edu (M.J. Hoffmann).

https://doi.org/10.1016/j.oceram.2022.100319
Received 29 September 2022; Received in revised form 28 November 2022; Accepted 2 December 2022
Available online 5 December 2022

2. Experimental

2.1. Raw materials

For preparation of the composite materials the following raw powders are used:

- Tantalum powder from haines & maassen Metallhandelsgesellschaft mbH, Germany,
- Alumina powder CT9FG from Almatis GmbH in Ludwigshafen, Germany, referred to as CT9FG,
- Alumina powder Alodur WRG from Imerys Fused Minerals Zschornewitz GmbH in Gräfenhainichen, Germany, referred to as Alodur.

The different powders are also used in other publications related to this work [1,2,7–11]. Both alumina raw powders differ in particle size and are used to investigate the influence of starting powder particle size on microstructural and electrical properties. The characteristic particle size values d_{10}, d_{50} and d_{90} are given in Table 1. According to manufacturers the purity of Alodur is stated to be $\geq$ 99.6% and CT9FG $\geq$ 99.5% with impurities of Fe_2O_3, Na_2O and SiO_2. Used Ta raw powder is reported to have a purity $\geq$99.95%.

Laser scanning and SEM micrographs in Fig. 1 show the differences of the used raw powders tantalum, Alodur and CT9FG. Ta shows coarse particles with round edges and also a fine-grained fraction in the raw powder. Alodur also shows coarse particles but compared to Ta the particles edges are sharper and no fine-grained fraction is present. Compared to the alumina Alodur, CT9FG shows small particles. In addition to the fine particles CT9FG contains agglomerates and aggregates within the raw powder, also visible in Fig. 1.

The XRD-pattern in Fig. 2 shows that the Ta raw powder has high purity and no secondary phases were detected.

2.2. Sample preparation

First, Al_2O_3–Ta-powder mixtures with varying metal content between 5 and 80 vol.-% Ta are produced from the raw powders. This is realized by a dry-mixing process, using a Turbular Tumbler type T2C from WAB AG Maschinenfabrik, Basel, Switzerland.

Then, sample preparation is done using a Field Assisted Sintering device type HP D 25/1 by FCT Systeme GmbH, Frankenblick, Germany. As described in other publications a big difference of FAST compared to conventional sintering is the additional application of axial pressure during the sintering process. As a result, even materials that cannot be densified using conventional sintering techniques can be processed with low remaining porosity after sintering. Another advantage of FAST is the possibility of applying high heating-rates of up to several hundred K/min and thus the processing time is reduced significantly [12–16]. The working principles and mechanisms as well as the setup and parameters used in this work are described in Ref. [7].

The samples are heated with a rate of 100 K/min up to 1600 °C and the temperature was hold for 5 min while at the same time an axial pressure of 50 MPa is applied. After the dwell time the pressure is released, and the samples are cooled with a rate of 100 K/min to 25 °C.

Table 1
Characteristic particle sizes d_{10}, d_{50} and d_{90} of the used raw powders Ta, CT9FG and Alodur [7,11].

Starting powder	d_{10} (μm)	d_{50} (μm)	d_{90} (μm)
Tantalum	6.0	32.2	68.3
Alodur	44.8	95.8	162.4
CT9FG	0.8	4.4	11.9

2.3. Microstructural analysis

Samples are prepared by grinding and polishing of representative cross sections up to a polishing step using diamond suspension with a particle diameter of 0.25 μm. The microstructure is analyzed using a digital microscope type VHX-6000 and a laser scanning microscope type VK-X200, both from Keyence Deutschland GmbH, Neu-Isenburg, Germany. The microstructural findings are then linked to the macroscopic properties.

Density of the samples is measured using Archimedes principle.

2.4. Electrical conductivity

After sintering the refractory composite materials are investigated regarding their electrical conductivity and their density, depending on the composition and the used raw powders. Sample preparation for the characterization of electrical properties is described in Refs. [1,7]. For the electrical conductivity measurement surfaces of sintered samples were ground using 600P SiC paper. After grinding the samples were sputter coated with gold using a Quorum Q150T ES and an additional layer of PELCO colloidal silver paste was added to ensure a continuous electrode over the whole sample surface, also for the porous materials investigated here. For anisotropy investigations the samples were cut using a cutting device type WOCO 50P by Hommel. After cutting the surfaces were prepared as mentioned before. Electrical conductivity measurements are performed using a four-point-measurement setup, also used and described in Refs. [1,2,7].

3. Results and discussion

3.1. Microstructural analysis

The results of the density measurements after sintering are shown in Fig. 3. As can be seen for the material Ta-CT9FG, densification by FAST results in almost dense samples with relative densities in the range of 98–100%, almost independent of the material composition, except for pure Ta which reveals a relative density of 96.2%.

In contrast to Ta-CT9FG, Ta-Alodur shows a strong dependency of the densification behavior on the metal/ceramic ratio. For pure Alodur a relative density of 80.1% is obtained. Density constantly increases with increasing metal content up to a value of 96.2% relative density for pure tantalum. The reduced densification when using the coarse-grained Alodur can be explained by the lower sintering activity of the coarse alumina particles compared to CT9FG. By increasing the sintering temperature, applied pressure and/or dwell time it might be possible to achieve higher densities of the Ta-Alodur composites [17].

Laser scanning micrographs of the samples Ta-CT9FG and Ta-Alodur with a material composition of 20 vol.-% Ta and 80 vol.-% Al_2O_3 are shown in Fig. 4, exemplarily for all compositions with a Ta-content between 5 and 80 vol.-%.

The micrographs show, that the microstructure of the Ta–Al_2O_3 composites is strongly dependent on the alumina particle size. The bright areas are the refractory metal, Ta. The grey areas correspond to the alumina while the darker/black areas are pores as well as remainings from the sample preparation process (e.g. breakouts from sample surface, residues of polishing media).

For Ta-CT9FG, the material shows the Ta-particles to be embedded in the fine-grained Al_2O_3 matrix and separated from each other. Here, a coarse-grained, as well as a very fine-grained fraction of Ta is visible in the micrographs.

The material system Ta-Alodur shows different microstructural features. Porosity is strongly increased to a value of 11.6% compared to the fine-grained alumina CT9FG with a porosity of 1.7% and the Alodur particles seem to keep their original shape during the sintering. Also, the Ta-particles do not seem to be separated from each other by a surrounding, isolating alumina matrix. The Ta-particles are heavily

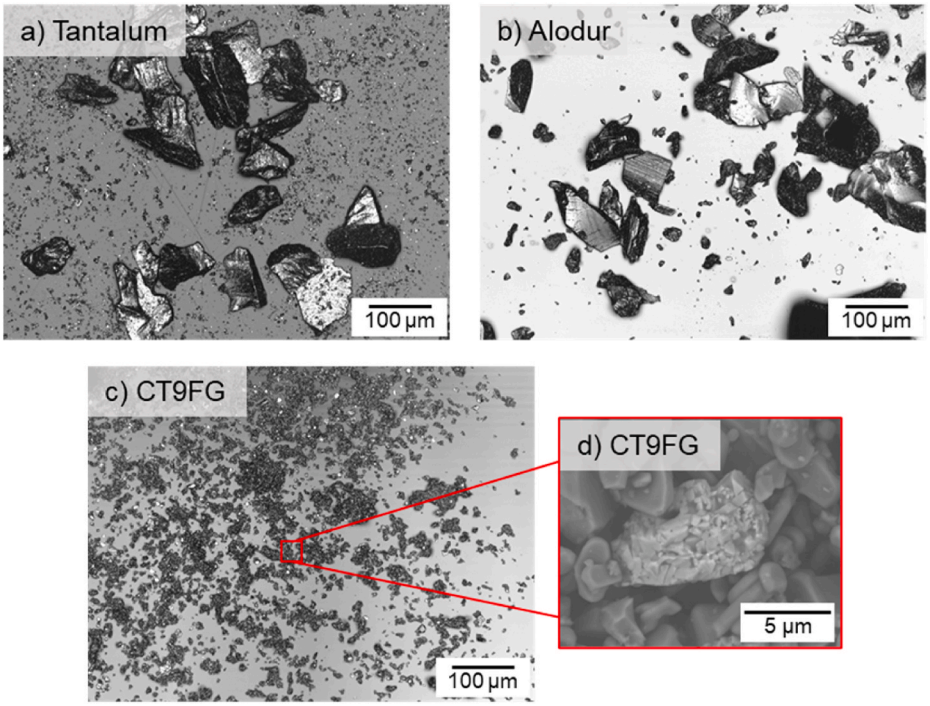

Fig. 1. Laser scanning micrographs of the used a) tantalum, b) Alodur and c) CT9FG raw powders and SEM micrograph of d) CT9FG agglomerate [7].

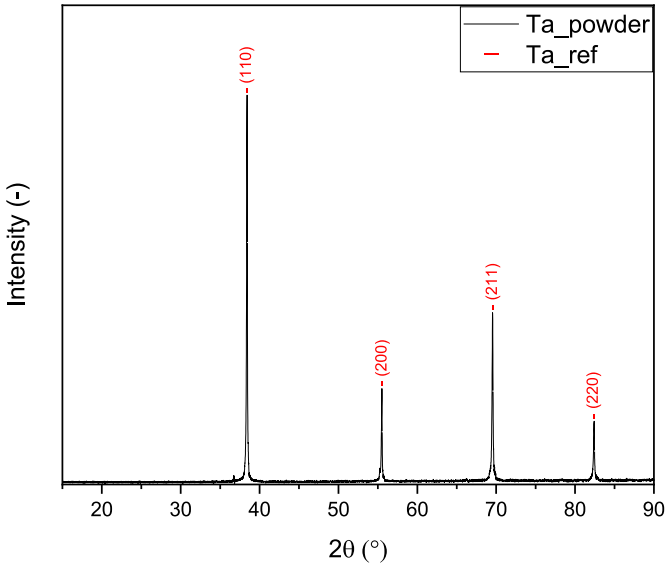

Fig. 2. XRD-pattern of Ta raw powder including reference pattern.

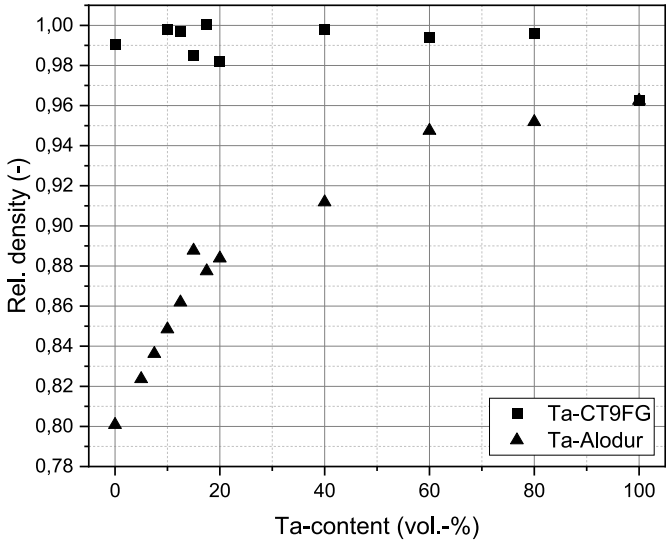

Fig. 3. Comparison of relative density of Ta-CT9FG and Ta-Alodur composite materials with different compositions.

deformed during the pressure-assisted densification process and squeezed into the pores between coarse Al_2O_3-particles. By this, the probability of generation of a continuous Ta-network through the composite is increased.

It is also noticeable, that for both material systems, the Ta particles seem to be elongated resulting in an anisotropic microstructure.

Fig. 5 shows representative cross sections of the materials Ta-CT9FG and Ta-Alodur for a composition of 40 vol.-% Ta and 60 vol.-% Al_2O_3. The schematic image on the left indicates the orientation of the examined cross sections relative to the axial pressure direction during the FAST process.

The micrographs in Fig. 5 indicate that the Ta-particles are elongated in a direction perpendicular to the axial pressure direction. As a result, some kind of texture effect is visible. This finding is important when it comes to mechanical as well as electrical properties, potentially leading to anisotropic material behavior [13].

3.2. Electrical conductivity

Fig. 6 shows the results of the electrical conductivity measurements in combination with the sample densities. Here, the measurement direction is parallel to the pressure direction during FAST. For both composites an increase in electrical conductivity with increasing Ta-content can be found. For low metal-contents up to 40 vol.-% Ta the material system Ta-Alodur shows a faster increase in electrical conductivity compared to the fine-grained system Ta-CT9FG. For higher metal contents of 60 and 80 vol.-% Ta the measured values are similar.

The percolation threshold of Ta-CT9FG is found to be between 12.5

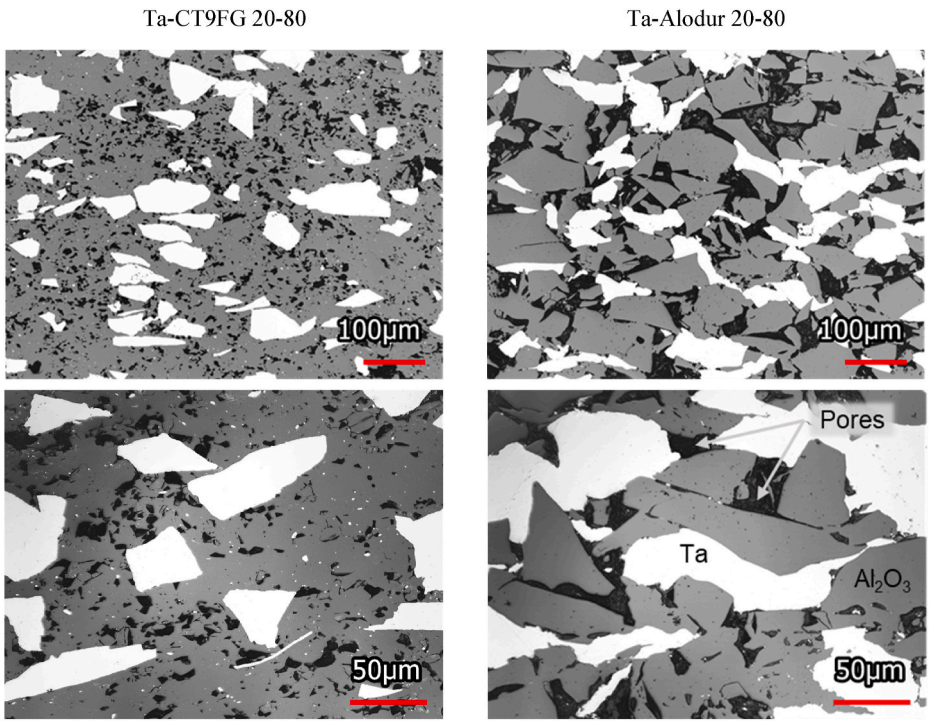

Fig. 4. Laser scanning microscope micrographs of Ta-CT9FG (left) and Ta-Alodur (right) with different magnifications (upper and lower micrographs) for a material composition of 20 vol.-% Ta and 80 vol.-% Al_2O_3.

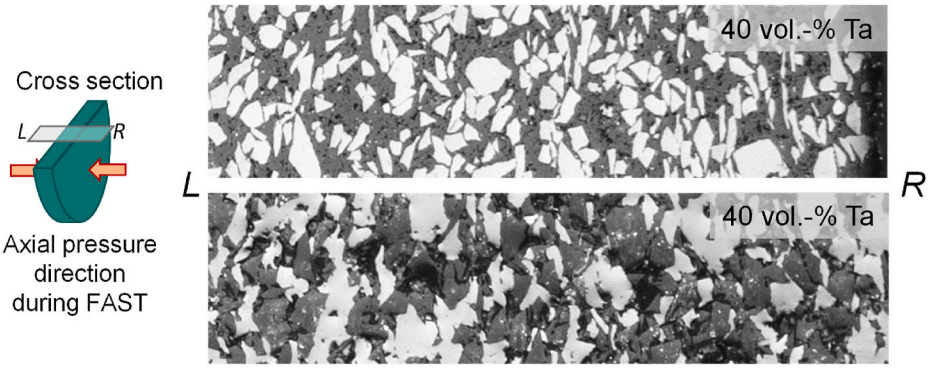

Fig. 5. Digital microscope micrographs of representative cross-sections of Ta-CT9FG (above) and Ta-Alodur (below) composites with orientation perpendicular to the pressure direction. Both materials had a composition of 40 vol.-% Ta and 60 vol.-% Al_2O_3.

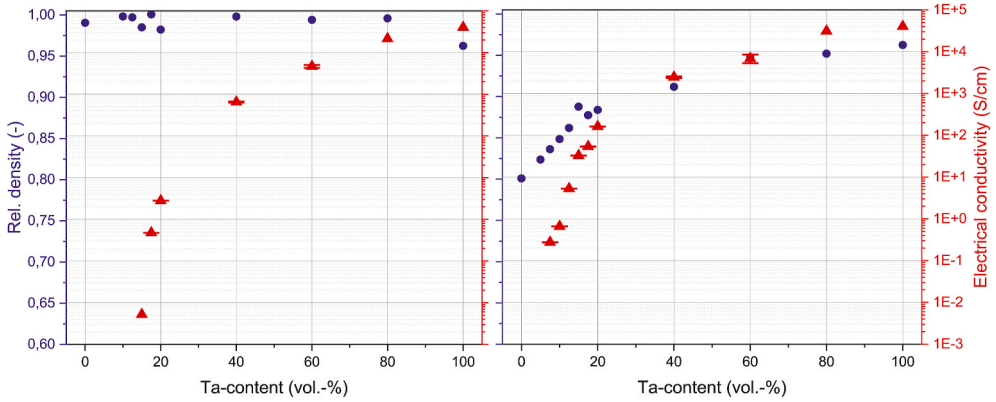

Fig. 6. Relative density and electrical conductivity of Ta-CT9FG (left) and Ta-Alodur (right) composites with varying metal contents.

and 15 vol.-% Ta. Near the percolation threshold the electrical conductivity sharply increases for small increases in metal content and stabilizes towards higher Ta-contents. These findings are in good agreement with percolation theory [18–23].

Ta-Alodur shows a percolation threshold between 5 and 7.5 vol.-% Ta, which is a decrease in metal content of about 7.5 vol.-% compared to the use of fine-grained alumina starting powder CT9FG.

In literature it is stated that electrical conductivity is dependent on material density, which in case of the investigated materials here does not seem to be the predominant factor [24–26]. In this study, the effect of particle shape seems to outrun the effect of porosity. According to literature, particle shape is another important factor in terms of formation of a conductive network through a composite material. It is stated that for increasing aspect ratio of electrically conductive particles within an isolating matrix, the percolation threshold decreases. This seems to be the predominant factor in case of Ta-Alodur, due to the deformation of the Ta-particles during the FAST-process resulting in higher aspect ratios and an increasing generation of an electrically conductive network [18–21,23]. The most important factor in terms of electrical conductivity still is the amount of conductive phase in the composite material, in this case the volume content of refractory metal tantalum.

In addition to the deformation of the Ta particles during densification, a texture can be seen in the microstructure with particles elongated perpendicular to the axial pressure direction during FAST. Therefore, the electrical conductivity was measured in three different directions relative to the applied pressure direction. The results are shown in Fig. 7.

The results reveal for all material compositions and both material systems a slightly smaller electrical conductivity along the a-axis, compared to the b- and c-axis.

This anisotropy is important and must be considered as design parameter for composite components for which a specific conductivity is required in the application.

4. Summary

$Ta–Al_2O_3$ composites were successfully processed using Field Assisted Sintering Technique (FAST). For a given Ta-content, it could be shown that the particle size of the alumina raw powders had a significant influence on microstructural development and electrical conductivity. The relative densities of fine-grained Ta-CT9FG composites were found to be almost independent of the Ta-content with >98% for all investigated samples, while the relative densities of Ta-Alodur composites constantly increased from 82% for the sample with 5% Ta to 95.2% for sample with 80% Ta.

There were also pronounced differences in the percolation: the fine-grained $Ta–Al_2O_3$ composite revealed the threshold for compositions in the range of 12.5–15 vol.-% Ta, in contrast to the coarse-grained Ta-Alodur composites which showed a reduced threshold between 5 and 7.5 vol.-% Ta. The reduction of percolation threshold can be attributed to a change in aspect ratio of the Ta particles as a result of FAST processing as evidenced by microstructural images. It indicates the formation of a metal network within the coarse-grained composite at lower metal contents compared to the fine-grained composite. Both material systems show an increase of electrical conductivity with an increase in metal content.

The microstructural analysis shows an anisotropy due to the applied axial pressure during densification. Ta particles were deformed and elongated in a direction perpendicular to the axial pressure direction. This anisotropy resulted in slightly smaller electrical conductivities parallel to the pressure direction, compared to electrical conductivities measured in directions perpendicular to it. The influence of anisotropy on percolation threshold has to be considered in terms of electrical conductivity of the composite materials and therefore will be part of future investigations. Also, passivation layers and interfacial reactions, as published in Refs. [27,28] are part of ongoing research.

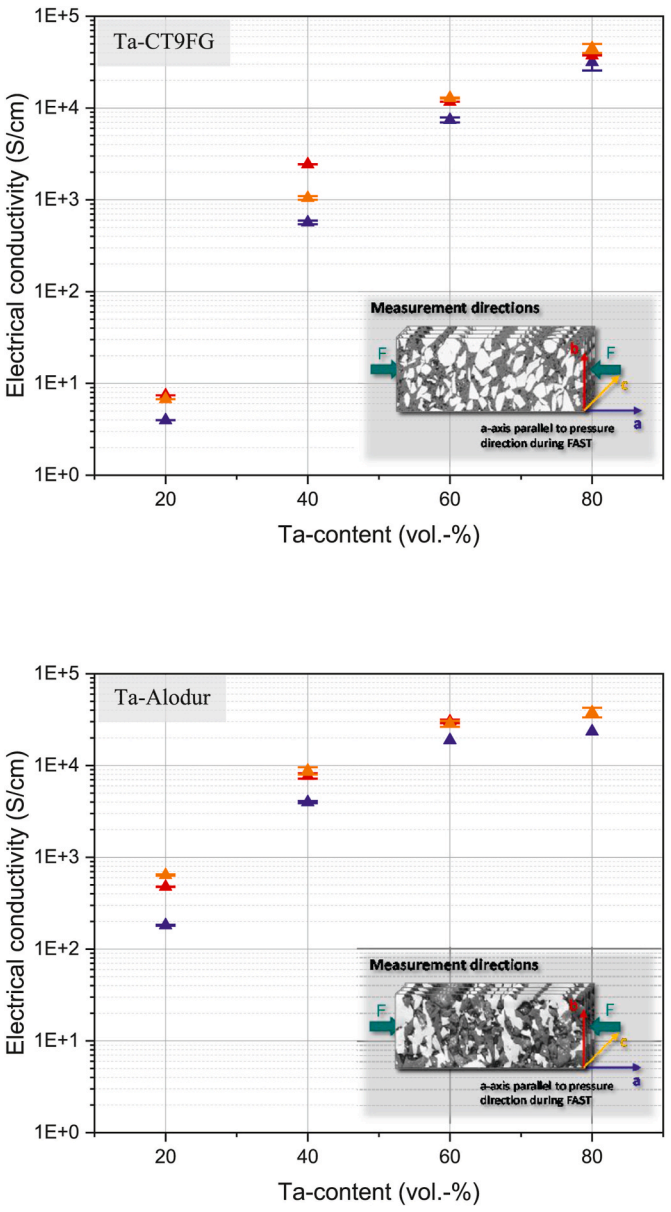

Fig. 7. Electrical conductivity of Ta-CT9FG (above) and Ta-Alodur (below) composites with different Ta-contents in different measurement directions relative to axial pressure direction during FAST process. a-axis (blue) parallel, b- (red) and c-axis (orange) perpendicular to pressure direction. (For interpretation of the references to colour in this figure legend, the reader is referred to the Web version of this article.)

The results are the basis to design a novel class of porous and heatable refractory composites with tailored microstructures and electrical conductivities prepared by a two-step processing route. For example, materials with high density are of interest for the preparation of dense composite particles by crushing to create designed microstructures for specific applications by re-sintering of the crushed particles. In addition, analysis of the percolation threshold found the lowest amount of metal needed to establish electrical conductivity, making it possible to create the most cost-efficient material by reducing costs of raw materials, in this case the tantalum.

Declaration of competing interest

The authors declare that they have no known competing financial interests or personal relationships that could have appeared to influence

the work reported in this paper.

Acknowledgements

This research was funded by the German Research Foundation (DFG) within the Research Unit FOR 3010 (Project number: 416817512).

References

[1] T. Zienert, et al., Synthesis of niobium-alumina composite aggregates and their application in coarse-grained refractory ceramic-metal castables, Materials 14 (21) (Oct. 2021) 6453, https://doi.org/10.3390/ma14216453.
[2] T. Zienert, M. Farhani, S. Dudczig, C.G. Aneziris, Coarse-grained refractory composites based on Nb-Al2O3 and Ta-Al2O3 castables, Ceram. Int. 44 (14) (2018) 16809–16818, https://doi.org/10.1016/j.ceramint.2018.06.116.
[3] C.G. Aneziris, M. Hampel, Microstructured and electro-assisted high-temperature wettability of MgO in contact with a silicate slag-based on fayalite, Int. J. Appl. Ceram. Technol. 5 (5) (Sep. 2008) 469–479, https://doi.org/10.1111/j.1744-7402.2008.02223.x.
[4] A. Weidner, Y. Ranglack-Klemm, T. Zienert, C.G. Aneziris, H. Biermann, Mechanical high-temperature properties and damage behavior of coarse-grained alumina refractory metal composites, Materials 12 (23) (2019) 3927, https://doi.org/10.3390/ma12233927.
[5] W.E. Lee, S. Zhang, M. Karakus, Refractories: controlled microstructure composites for extreme environments, J. Mater. Sci. 39 (22) (Nov. 2004) 6675–6685, https://doi.org/10.1023/B:JMSC.0000045599.84988.9e.
[6] S. Schafföner, C.G. Aneziris, Pressure slip casting of coarse grain oxide ceramics, Ceram. Int. 38 (1) (Jan. 2012) 417–422, https://doi.org/10.1016/j.ceramint.2011.06.064.
[7] B. Kraft, S. Wagner, K.G. Schell, M.J. Hoffmann, Field-assisted sintering of Nb–Al 2 O 3 composite materials and investigation of electrical conductivity, Adv. Eng. Mater. 24 (8) (Aug. 2022), 2200063, https://doi.org/10.1002/adem.202200063.
[8] T. Zienert, et al., Characterization of sintered niobium–alumina refractory composite granules synthesized by castable technology, Adv. Eng. Mater. 24 (8) (Aug. 2022), 2200407, https://doi.org/10.1002/adem.202200407.
[9] E. Storti, M. Neumann, T. Zienert, J. Hubálková, C.G. Aneziris, Full and hollow metal–ceramic beads based on tantalum and alumina produced by alginate gelation, Adv. Eng. Mater. 24 (8) (Aug. 2022), 2200381, https://doi.org/10.1002/adem.202200381.
[10] G. Günay, T. Zienert, D. Endler, C.G. Aneziris, H. Biermann, A. Weidner, High-temperature compressive behavior of refractory alumina–niobium composite material, Adv. Eng. Mater. 24 (8) (Aug. 2022), 2200292, https://doi.org/10.1002/adem.202200292.
[11] D. Endler, T. Zienert, V. Roungos, J. Hubálková, P. Gehre, C.G. Aneziris, Low shrinkage, coarse-grained tantalum–alumina refractory composites via cold isostatic pressing, Adv. Eng. Mater. 24 (8) (Aug. 2022), 2200754, https://doi.org/10.1002/adem.202200754.
[12] M. Zhou, L. Ren, G. Quan, M. Gupta, Solid phase processing of metal matrix composites, in: Encyclopedia of Materials: Composites, Elsevier, 2021, pp. 173–196.
[13] O. Guillon, et al., Field-assisted sintering technology/spark plasma sintering: mechanisms, materials, and technology developments, Adv. Eng. Mater. 16 (7) (2014) 830–849, https://doi.org/10.1002/adem.201300409.
[14] M.K.L. Feuchter, Investigations on Joule Heating Applications by Multiphysical Continuum Simulations in Nanoscale Systems, 2014.
[15] J. Räthel, M. Herrmann, W. Beckert, Temperature distribution for electrically conductive and non-conductive materials during Field Assisted Sintering (FAST), J. Eur. Ceram. Soc. 29 (8) (2009) 1419–1425, https://doi.org/10.1016/j.jeurceramsoc.2008.09.015.
[16] K. Vanmeensel, A. Laptev, J. Hennicke, J. Vleugels, O. Van Der Biest, Modelling of the temperature distribution during field assisted sintering, Acta Mater. 53 (16) (2005) 4379–4388, https://doi.org/10.1016/j.actamat.2005.05.042.
[17] M.N. Rahaman, Ceramic Processing and Sintering, second ed., CRC Press Inc, Bosa Roca, 2003.
[18] M. Sahimi, A.G. Hunt, Complex Media and Percolation Theory, New York, first ed., Springer Science+Business Media, New York, 2021.
[19] R.G. Arenhart, G.M.O. Barra, C.P. Fernandes, Simulation of percolation threshold and electrical conductivity in composites filled with conductive particles: effect of polydisperse particle size distribution, Polym. Compos. 37 (1) (Jan. 2016) 61–69, https://doi.org/10.1002/pc.23155.
[20] Q. Xue, The influence of particle shape and size on electric conductivity of metal-polymer composites, Eur. Polym. J. 40 (2) (2004) 323–327, https://doi.org/10.1016/j.eurpolymj.2003.10.011.
[21] X. Jing, W. Zhao, L. Lan, Effect of particle size on electric conducting percolation threshold in polymer/conducting particle composites, J. Mater. Sci. Lett. 19 (5) (2000) 377–379, https://doi.org/10.1023/A:1006774318019.
[22] S.H. Yao, Z.M. Dang, M.J. Jiang, H.P. Xu, J. Bai, Influence of aspect ratio of carbon nanotube on percolation threshold in ferroelectric polymer nanocomposite, Appl. Phys. Lett. 91 (21) (2007), https://doi.org/10.1063/1.2817746.
[23] A.K. Sircar, T.G. Lamond, Effect of carbon black particle size distribution on electrical conductivity, Rubber Chem. Technol. 51 (1) (Mar. 1978) 126–132, https://doi.org/10.5254/1.3535720.
[24] N. Probst, E. Grivei, Structure and electrical properties of carbon black, Carbon N. Y. 40 (2) (Feb. 2002) 201–205, https://doi.org/10.1016/S0008-6223(01)00174-9.
[25] L.J. Kennedy, J.J. Vijaya, G. Sekaran, Electrical conductivity study of porous carbon composite derived from rice husk, Mater. Chem. Phys. 91 (2–3) (Jun. 2005) 471–476, https://doi.org/10.1016/j.matchemphys.2004.12.013.
[26] H. El Khal, A. Cordier, N. Batis, E. Siebert, S. Georges, M.C. Steil, Effect of porosity on the electrical conductivity of LAMOX materials, Solid State Ionics 304 (Jun. 2017) 75–84, https://doi.org/10.1016/j.ssi.2017.03.028.
[27] M.K. Eusterholz, et al., High-temperature ternary oxide phases in tantalum/niobium–alumina composite materials, Adv. Eng. Mater. 24 (8) (Aug. 2022), 2200161, https://doi.org/10.1002/adem.202200161.
[28] J. Gebauer, P. Franke, H.J. Seifert, Thermodynamic evaluation of the system Ta–O and preliminary assessment of the systems Al–Nb–O and Al–Ta–O, Adv. Eng. Mater. 24 (8) (Aug. 2022), 2200162, https://doi.org/10.1002/adem.202200162.